Int. J. Advanced Design and Manufacturing Technology, 2024, Vol. 17, No. 2, pp. 51-60

DOI: 10.30486/ADMT.2024.873789 ISSN: 2252-0406 https://admt.isfahan.iau.ir

Numerical Analysis of Time Dependent Temperature Distribution inside a Solar Greenhouse

Mahya Mohammadi*
Department of Mechanical Engineering,
K. N. Toosi University of Technology, Tehran, Iran
University of Waterloo, Waterloo, Ontario, Canada
E-mail: mahya.mohammadi@email.kntu.ac.ir
*Corresponding author

Cyrus Aghanajafi
Department of Mechanical Engineering,
K. N. Toosi University of Technology, Tehran,
E-mail: aghanajafi@kntu.ac.ir

Received: 23 January 2020, Revised: 4 June 2020, Accepted: 14 July 2020

Abstract: In the present study, a numerical model is developed to predict time-dependent temperature variations inside a solar greenhouse by solving the continuity, Navier-Stokes, and energy Equations using ANSYS Fluent. This paper considers all heat transfer mechanisms into and out of the greenhouse, including convection, radiation, and conduction. The surface-to-surface model and SIMPLE method are employed to analyse thermal radiation between surfaces within the greenhouse and to couple pressure and velocity in solving the flow-field Equations numerically, respectively. This study specifically investigates the unsteady temperature distribution within a solar greenhouse located in Makran, Iran (latitude: 25.3054°N, longitude: 60.6411°E). The numerical method of this study is validated by comparing its results with experimental data. The high accuracy demonstrated by this approach supports the conclusion that the model can effectively study the flow field and thermal behaviour inside solar greenhouses. It is demonstrated that fluctuating boundary conditions cause the thermal conditions inside the greenhouse to vary dynamically over time. The results depict the spatial variation of temperature distribution at different levels from the soil surface at 13:00 on the first and second days of modelling in Makran. These insights are expected to play a crucial role in improving greenhouse design and management practices in agriculture.

Keywords: Heat Transfer, Iran, Makran, Numerical Model, Surface-To-Surface Model, Solar Greenhouse, Time-Dependent Temperature Variations

Biographical notes: **Mahya Mohammadi** received her PhD in Mechanical Engineering from K. N. Toosi University of Technology in 2022. She completed a visiting period at the University of Waterloo, Canada. Currently. Her research interests focus on fluid mechanics and transfer phenomena, particularly their applications in cancer treatment modeling. **Cyrus Aghanajafi** is a Full Professor at K. N. Toosi University of Technology. He received his PhD in Mechanical Engineering from Tennessee State University, USA. His current research focuses on fluid mechanics, heat transfer, and thermodynamics.

Research paper

1 INTRODUCTION

Solar greenhouses are typically defined as enclosures that provide an appropriate environment to grow crops such as plants, flowers, and vegetables [1]. The solar greenhouse industry effectively uses renewable solar energy. There are two types of solar greenhouses: passive and active. In passive solar greenhouses, solar energy is used to heat water, concrete, or other heat-holding materials, with minimal human involvement in the self-regulated warming process [2]. The active system, however, requires electricity or another conventional source of energy [3].

Experimental studies of greenhouses are too expensive, and their results are only useful for specific conditions and geometry. Therefore, numerical models are needed to predict the temperature distribution inside greenhouses. Computational Fluid Dynamics (CFD) is a powerful tool to simulate the climatic conditions within greenhouses [4]. Okushima et al. [5] studied ventilation in greenhouses using CFD for the first time. They compared the results of the numerical method with experimental data [6]. This technique was not used for some time until Bot et al. [7] compared the CFD results of a two-span greenhouse simulation with data obtained by means of sonic anemometry.

CFD has been increasingly used in simulating greenhouse climatic conditions. Bartzanas et al. [8] studied the effect of an insect-proof screen (located in the side openings of a tunnel greenhouse) on airflow and temperature distribution using CFD. They found that airflow was reduced and the thermal gradient increased by using the insect screen. Molina-Aiz et al. [9] studied the effect of wind speed on the inner climatic conditions of the greenhouse using finite element method-based software. The continuity, momentum, energy, turbulent kinetic energy, and dissipation rate Equations were solved. They found that ventilation was a significant parameter affecting crop growth. Tong et al. [10] predicted the temperature distribution inside a Chinese solar greenhouse during three clear days followed by a cloudy day using the CFD method. Radiation, convection, and conduction heat transfer were all assumed in their study to present an accurate prediction. Rodriguez and Velazquez [11] demonstrated the capability of CFD in predicting climate control in a solar greenhouse, considering heat and mass transfer.

A system of Equations for heat and moisture transfer during the drying of copra in a solar greenhouse dryer was numerically solved using the finite difference method by Sadodin and Kashani [12]. Based on the results, it was concluded that this type of dryer can be used in rural areas without electricity grids, with an estimated payback period of about 2.3 years. Lokeswaran and Eswaramoorthy [13] validated their experimental results on natural convection in a solar greenhouse dryer using Fluent software. They solved the continuity, momentum, and energy Equations simultaneously using the SIMPLE scheme for pressure-velocity coupling.

Deiana et al. [14] investigated the effect of different building materials on the internal temperature of Chinese solar greenhouses throughout the entire cold season, using numerical methods. Chen et al. [15] studied the contribution of an active-passive ventilation wall with phase change material (PCM) in improving the north wall of a solar greenhouse, both numerically and experimentally. They demonstrated the effectiveness of the proposed wall by monitoring the increase in indoor air temperature, daily effective accumulative temperature, and soil temperature.

Tong and Christopher [16] investigated the effect of different parameters on the inner temperature distribution in a Chinese solar greenhouse through sensitivity analysis. He et al. [17] simulated a 2D model of a solar greenhouse using FLUENT to determine the best size for the back wall vent. The discrete ordinates radiation model was used to calculate coupled radiation and convective exchanges. They found that vents were the key factor affecting the greenhouse temperature distribution. Esmaeli and Roshandel [18] optimized the structural properties of a solar greenhouse based on a thermal model to minimize the deviation of the temperature from the suitable temperature range. They found that the optimized parameters are depended on the objective function, varying from year-round performance to seasonal or cultivation period performances.

In this study, a sophisticated numerical model is developed to simulate the climatic conditions within a solar greenhouse, with a specific focus on the thermal behaviour of a greenhouse located in Makran, Iran. This analysis is crucial for optimizing agricultural practices in the region. The model incorporates time-dependent boundary conditions, including solar insolation, sky temperature, outside air temperature, and outside air relative humidity. These parameters are accurately determined and implemented in the simulation software using a user-defined function (UDF) to ensure the precision of the numerical model. The research methodology includes a rigorous validation process, where the model's predictions are compared against experimental data to verify its accuracy. Another significant contribution of this research is providing detailed insights into the temperature distribution within the solar greenhouse in Makran, Iran.

2 MATERIALS AND METHODS

In the current study, a numerical model is employed to simulate the temperature distribution inside a solar

greenhouse. The model's geometry, computational domain, governing Equations, boundary conditions (BCs), effective properties of the layered surfaces, and numerical solution procedure are discussed in the following subsections.

2.1. Model Geometry and Computational Domain

Figure 1 shows the cross-sectional view of the greenhouse. The soil depth under the greenhouse is assumed to be 1.0 m. The greenhouse is modeled as two-dimensional.

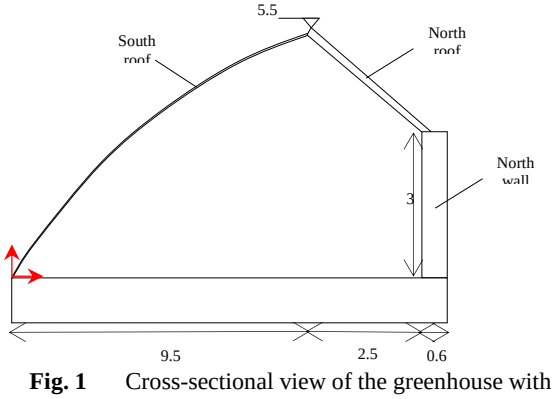

Fig. 1 Cross-sectional view of the greenhouse with dimensions [m].

2.2. Governing Equations

The system is simulated by discretizing space and time using the finite-volume method and solving the incompressible, unsteady, two-dimensional laminar conservation Equations for the velocity and temperature fields on an unstructured grid. The continuity, Navier-Stokes, and energy Equations are represented as [19]:

$$\frac{\partial U_i}{\partial x_i} = 0 \tag{1}$$

$$\rho \frac{\partial U_i}{\partial t} + \rho U_j \frac{\partial U_i}{\partial x_j} = -\frac{\partial p}{\partial x_i} + \frac{\partial}{\partial x_j}(2\mu S_{ji}) + \rho f_i \tag{2}$$

$$\rho \frac{\partial u}{\partial t} + \rho U_i \frac{\partial u}{\partial x_i} = -p \frac{\partial U_j}{\partial x_j} + \frac{\partial}{\partial x_j}(k \frac{\partial T}{\partial x_j} - q_r) + \Phi + Q \tag{3}$$

The vectors U_i and x_i are velocity and position, T is temperature, p is pressure, ρ is density, μ is molecular viscosity, f_i is body force per unit mass, u is the internal energy per unit mass (the most frequent form of u is $u = cdT$ for liquids and $u = c_v dT$ for gases where c_v is the specific heat at constant volume), k is thermal conductivity, Q is the heat source or sink, q_r is radiation term, Φ is dissipation rate, and S_{ji} is the strain rate tensor that can be written as follows [19]:

$$S_{ji} = \frac{1}{2}(\frac{\partial U_i}{\partial x_j} + \frac{\partial U_j}{\partial x_i}) \tag{4}$$

2.2.1. Solar Radiation Model

Solar radiation is a crucial factor influencing the indoor temperature and airflow distribution in a greenhouse. It is assumed that air does not participate in thermal radiation exchange. Thermal radiation heat transfer between surfaces inside the greenhouse is calculated using the Surface-to-Surface (S2S) model. This model can be used to account for radiation exchange in an enclosure with gray-diffuse surfaces. The energy exchange between two surfaces depends in part on their size, separation distance, and orientation. These parameters are accounted for by a geometric function called a view factor. The main assumption of the S2S model is that any absorption, emission, or scattering of radiation can be ignored; therefore, only surface-to-surface radiation needs to be considered for analysis [20].

The energy flux leaving a particular surface consists of emitted and reflected components. The amount of reflected energy flux depends on the incident energy flux from the surroundings, which can be described in relation to the energy flux from all other surfaces. The energy reflected from surface k is [21]:

$$q_{out,k} = \varepsilon_k \sigma T_k^4 + \rho_k q_{in,k} \tag{5}$$

Where $q_{out,k}$, ε_k, σ, ρ_k, and $q_{in,k}$ are energy flux leaving the surface, emissivity, Boltzmann's constant, transmissivity, and energy flux incident on the surface from the surroundings, respectively. The incident energy on a surface from another surface is directly determined by the surface-to-surface view factor, F_{jk}. The view factor F_{jk} represents the fraction of energy leaving surface k that reaches surface j.

The incident energy flux $q_{in,k}$ can be expressed in relation to the energy flux leaving all other surfaces as follows [21]:

$$A_k q_{in,k} = \sum_{j=1}^{N} A_j q_{out,j} F_{jk} \tag{6}$$

Where A_k is the area of surface k and F_{jk} is the view factor between surface k and surface j. For N surfaces, applying the view factor reciprocity relationship yields [20]:

$$A_j F_{jk} = A_k F_{kj} \; for j = 1,2,3,...,N \tag{7}$$

So that:

$$q_{in,k} = \sum_{j=1}^{N} F_{kj} q_{out,j} \tag{8}$$

Therefore:

$$q_{out,k} = \varepsilon_k \sigma T_k^4 + \rho_k \sum_{j=1}^{N} F_{kj} q_{out,j} \tag{9}$$

Which can be written as [21]:

$$J_k = E_k + \rho_k \sum_{j=1}^{N} F_{kj} J_j \tag{10}$$

Where J_k represents the radiosity (energy given off) of surface k, and E_k represents the emissive power of surface k. This forms N Equations, which can be reformulated into matrix form as follows [20]:

$$KJ = E \tag{11}$$

Where K is a $N \times N$ matrix, J is the radiosity vector, and E is the emissive power vector. Equation (11) is referred to as the radiosity matrix Equation. The view factor between two finite surfaces i and j is defined as [20]:

$$F_{ij} = \frac{1}{A_i} \int_{A_i} \int_{Aj} \frac{\cos\theta_i \cos\theta_j}{\pi r^2} \delta_{ij} dA_i dA_j \tag{12}$$

Where δ_{ij} is evaluated by the visibility of dA_j to dAi . $\delta_{ij} = 1$ if dA_j is visible to dAi and 0 otherwise.

2.3. BCS and Effective Properties of The Layered Surfaces

The thermal radiation heat transfer between the inner surfaces, as well as between the outside surfaces and the sky, is considered due to the temperature difference. The S2S model is applied to calculate the radiation heat transfer between surfaces inside the greenhouse. Natural convection inside the greenhouse, convection between the outside air and the greenhouse surfaces, condensation on the cover, and air filtration are all considered.

The sky temperature is calculated as [22]:

$$T_{sky} = \varepsilon_{sky}^{0.25} (T_{ao} + 273) \tag{13}$$

$$\varepsilon_{sky} = 0.74 + 0.006 T_{dp} \tag{14}$$

Where T_{ao} is the outside temperature, ε_{sky} is the sky emissivity. The dew point temperature, T_{dp}, is a function of the relative humidity and the outside air temperature, and an empirical relationship is used [23]:

$$T_{dp} = (112 + 0.9T_{ao}) RH^{0.125} + (0.1T_{ao} - 112) \tag{15}$$

RH is the relative humidity outside the greenhouse. T_{ao} is in °C in "Eq. (15)". The air temperature and relative humidity outside the greenhouse used in this study are shown in "Figs. 2 and 3".

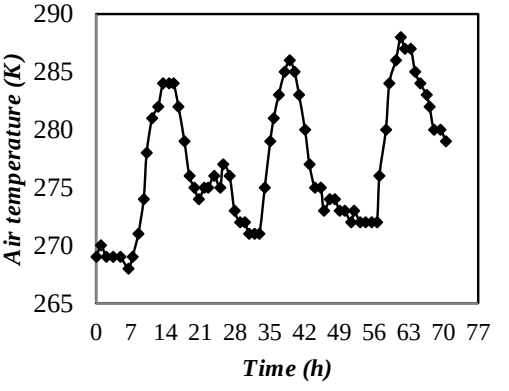

Fig. 2 Air temperature outside [10].

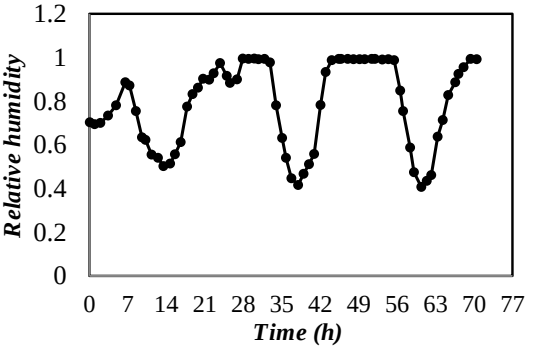

Fig. 3 Air relative humidity [10].

The solar radiation reaching the inner surfaces includes both beam solar radiation and diffuse solar radiation. The beam solar radiation fluxes on the inner surfaces are specified by [10]:

$$q_{b,ground} = q_b \tau_b \tag{16}$$

$$q_{b,northwall} = \frac{\cos\theta_w}{\cos\theta_z} q_{b,ground} \tag{17}$$

$$q_{b,northroof} = \frac{\cos\theta_r}{\cos\theta_z} q_{b,ground} \tag{18}$$

Where q_b is the solar beam radiation flux on a horizontal

surface outside in w/m^2, depicted in "Fig. 4". τ_b, θ_z, θ_w and θ_r represent the south roof cover film transmittance for beam radiation, angles of incidence on the horizontal (soil), north wall, and north roof surfaces, respectively. The view factors required for calculating the diffuse solar radiation on the inner surfaces are provided in [10]:

$$\eta_{ab,bc} = \frac{l_{ab} + l_{bc} - l_{ac}}{2l_{ab}} \tag{19}$$

$$\eta_{ab,ad} = \frac{l_{ab} + l_{ad} - l_{bd}}{2l_{ab}} \tag{20}$$

$$\eta_{ab,cd} = \frac{l_{bd} + l_{ac} - l_{bc} - l_{ad}}{2l_{ab}} \tag{21}$$

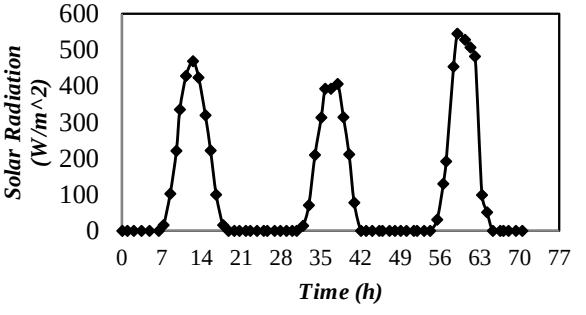

Fig. 4 Total solar radiation outside on a horizontal surface [10].

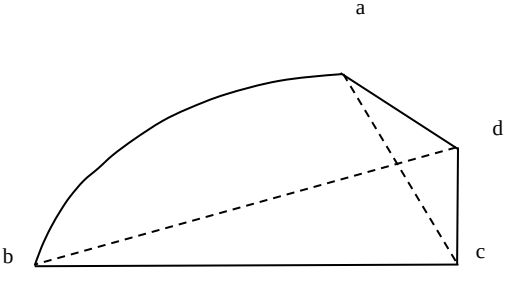

Fig. 5 Scheme of the surface view factor [10].

Figure 5 shows the scheme of the surface view factors. The calculation of diffuse solar radiation fluxes to the inner surfaces is described in [10]:

$$q_{d,ground} = q_{d,southroof}\tau_d\eta_{ab,bc} \tag{22}$$

$$q_{d,northwall} = q_{d,southroof}\tau_d\eta_{ab,cd} \tag{23}$$

$$q_{d,northroof} = q_{d,southroof}\tau_d\eta_{ab,ad} \tag{24}$$

Where $q_{d,southroof}$ is the diffuse radiation flux to the south roof surface in w/m^2. τ_d is the south roof cover film transmittance for diffuse radiation. The diffuse radiation flux on a horizontal surface is assumed to be 20% of the total solar radiation [10].
The solar radiation flux incident on the south roof can be calculated as [24]:

$$q_{sf,o} = R_b q_b + R_d q_d + R_{re}(q_b + q_d) \tag{25}$$

Where $q_{sf,o}$ is the total solar radiation flux outside the south roof in w/m^2. q_b, q_d, R_b, R_d, and R_{re} represent beam radiation, diffuse radiation, the ratio of the beam radiation incident flux on the south roof to that on the horizontal surface, the ratio of the diffuse radiation incident flux on the south roof to that on the horizontal surface, and the reflected component, respectively. R_b, R_d, and R_{re} can be calculated as [24]:

$$R_b = \frac{\cos\theta_{sf}}{\cos\theta_z} \tag{26}$$

$$R_d = \frac{1+\cos\beta}{2} \tag{27}$$

$$R_{re} = \alpha\left(\frac{1-\cos\beta}{2}\right) \tag{28}$$

Where θ_{sf}, θ_z, β, and α represent the angles of incidence relative to the south roof, the angles of incidence relative to the horizontal surface, the angle between the south roof plane and the horizontal plane, and the reflection coefficient of the ground, respectively. According to "Fig. 6", the incidence angle of the sloped plane is determined as [25]:

$$\cos\theta = \sin\delta\sin\phi\cos\beta - \sin\delta\cos\phi\sin\beta\cos\gamma + \cos\delta\cos\phi \cos\beta\cos\omega + \cos\delta\sin\phi\sin\beta\cos\gamma\cos\omega + \cos\delta\sin\beta\sin\gamma\sin\omega \tag{29}$$

Where δ, ϕ, γ, and ω are declination, latitude, solar azimuth, and hour angel, respectively. Declination is determined by using "Fig. 7". ω and γ can be calculated as [25]:

$$\omega = 15^{\circ}(Solartime - 12) \tag{30}$$

$$Solar\ time = Standard\ time + \frac{4(local\ solar\ time - longitude) + E}{60} \quad (31)$$

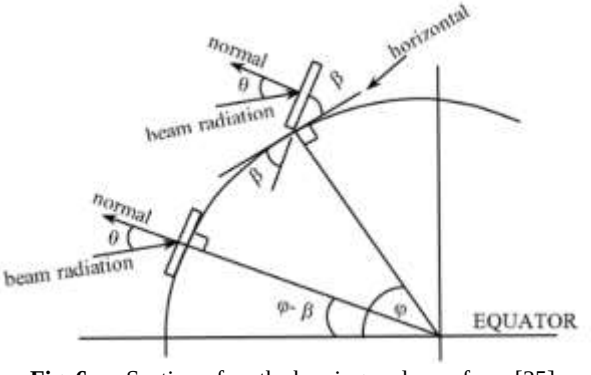

Fig. 6 Section of earth showing, redrawn from [25].

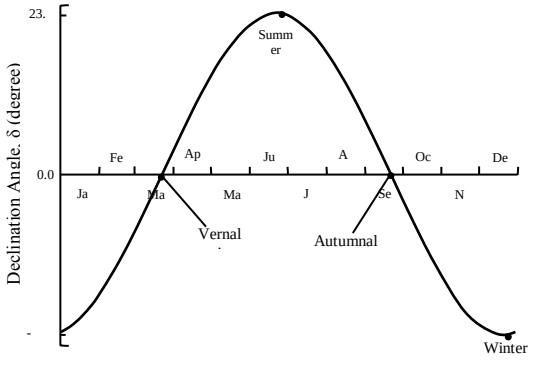

Fig. 7 Variation of the declination angel, redrawn from [26].

$$E = 229.2(0.000075 + 0.001868\cos B - .032077\sin B - .014615\cos 2B - .04089\sin 2B) \quad (32)$$

$$B = \frac{(n-1)360}{365} \quad (33)$$

Where n is the number of days since the start of the year.

$$\gamma = sin(\omega)\left|cos^{-1}\left(\frac{cos\,\theta_z\,sin\,\phi - sin\,\delta}{sin\,\theta_z\,cos\,\phi}\right)\right| \quad (34)$$

Condensation occurred on the inside south roof surface during a certain time range [10]. The latent heat flux (W/m^2) due to condensation, as given by Garzoli [27], is:

$$q_{condensation} = \frac{h_c L(w_a - w_c)}{c_p} \quad (35)$$

Where h_c is the inside surface heat transfer coefficient, $7.2(W/m^2K)$ [28]. c_p is the specific heat of air (J/kgK), L is the latent heat of vaporization (J/kg), and w_a and w_c are the humidity ratio in the greenhouse air and the humidity ratio of air saturated at the cover temperature, respectively, with [10]:

$$w_a = \frac{RH}{100}(0.004055 + 0.0001152t_a + 0.00002167t_a^2) \quad (36)$$

$$w_c = 0.004055 + 0.0001152t_c + 0.00002167t_c^2 \quad (37)$$

Where RH is the relative humidity of the greenhouse air, t_a is the greenhouse air temperature in °C and, t_c is the cover temperature in °C.

The total leakage heat losses due to air infiltration are the sum of the sensible and latent leakage losses [29]:

$$q_{\inf,s} = \frac{NV\rho c_p \Delta T}{A_{enclosure}} \quad (38)$$

$$q_{\inf,l} = \frac{NV\rho L \Delta\omega}{A_{enclosure}} \quad (39)$$

Where V, ρ, ΔT, and $\Delta\omega$ represent the volume, air density, air temperature difference between the inside and outside of the greenhouse $(10K)$, and air humidity ratio difference between the inside and the outside of the greenhouse, respectively.

The actual physical properties of the layered structures used in this study are listed in "Table 1".

2.4. Numerical Solution Procedure

The geometry is created and the grid is generated with the aid of GAMBIT software. The governing Equations are solved numerically using ANSYS FLUENT 14. The unsteady boundary conditions of the greenhouse are implemented via a UDF. The momentum and energy Equations are solved using first-order upwind discretization, while the pressure is solved using standard discretization. The SIMPLE method is employed for pressure-velocity coupling. The convergence criterion is set to 10^{-6} for the energy Equation and 10^{-3} for the other Equations. Additionally, a mesh-free solution is considered.

Table 1 Effective properties of the layered surfaces [10]

Location	Layers thickness, mm	Density, $\frac{kg}{m^3}$	Specific heat, $\frac{J}{kgK}$	Thermal conductivity, $\frac{W}{mK}$	Emissivity
South roof day time	0.12	1400	1045	0.17	0.9
South roof night time	20	107.8	819	0.03	0.9
North wall inside layer	360	1800	1050	0.81	0.93
North wall middle layer	120	6.9	1329	0.03	
North wall outside layer	120	1800	1050	0.81	0.93
North roof	200	555.8	1091	0.06	0.91
Soil	1000	2050	1010	0.6	0.96

3 RESULTS

The present study is validated by comparing the results with the experimental data of Tong et al. [10]. Figure 8 shows the simulated and measured temperature distributions (K) at 13:00 on February 20, 2004 [10].

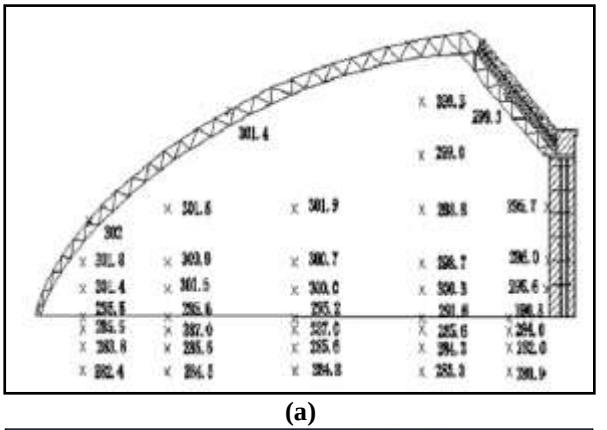

(a)

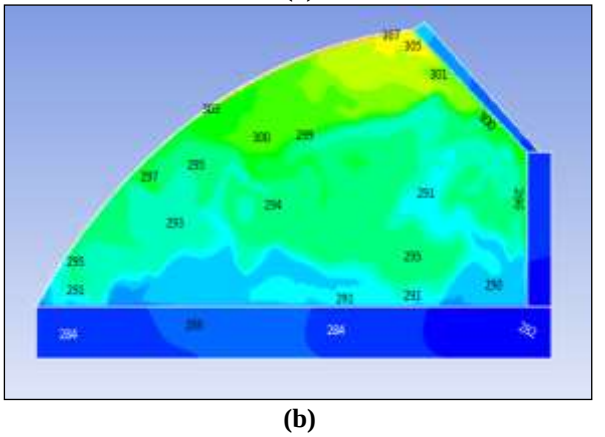

(b)

Fig. 8 Temperature distribution (K): (a): experimental data [10], and (b): numerical result.

As seen in "Fig. 8", there is a slight difference between the numerical results and the experimental data. It is concluded that the numerical method used is accurate. Some simplifications are considered in this study; for example, the average properties are considered for the layered structures. The existing difference may be due to these simplifications.

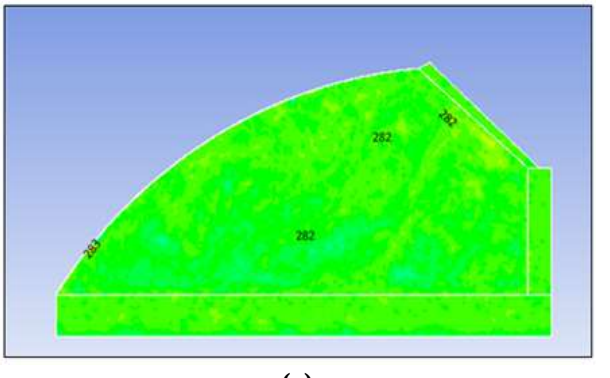

(a)

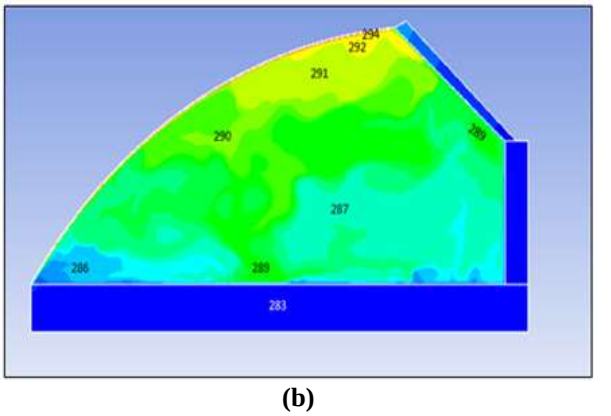

(b)

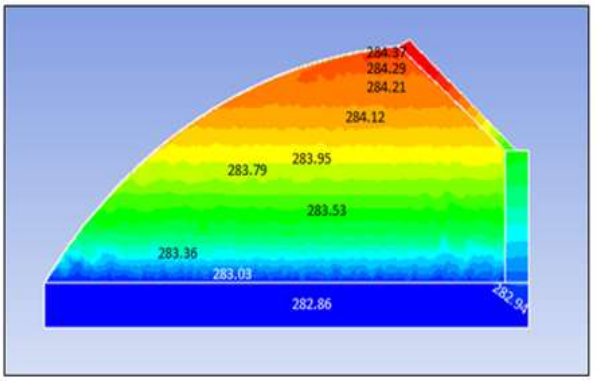

(c)

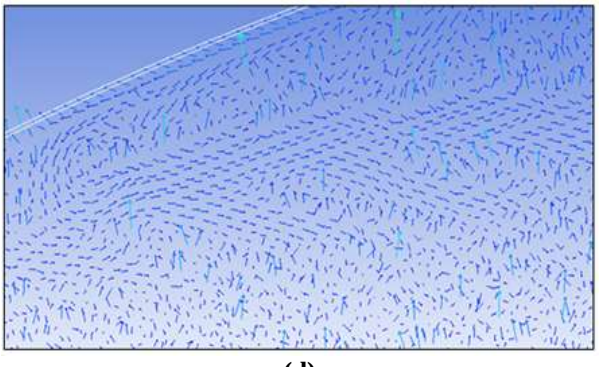

(d)

Fig. 9 Temperature distribution (K) at: (a): 8:00, (b): 13:00, and (c): 22:00 (first day). (d): velocity vector at 13:00 near the south roof.

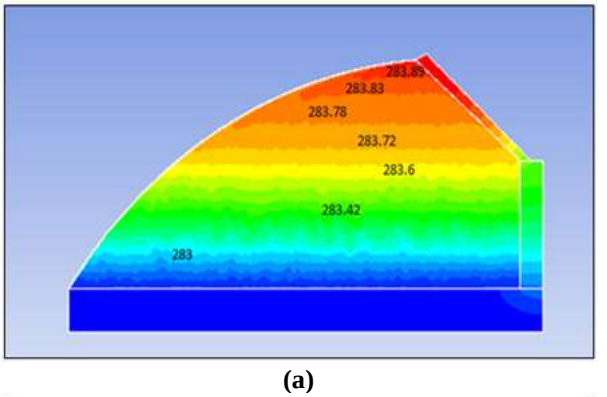

(a)

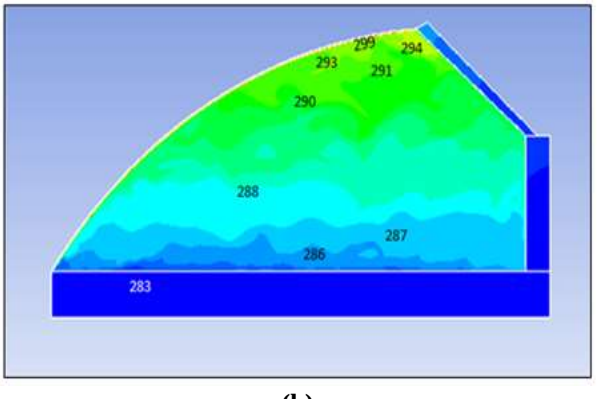

(b)

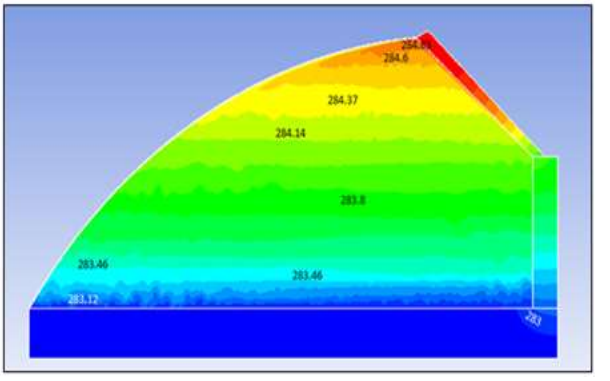

(c)

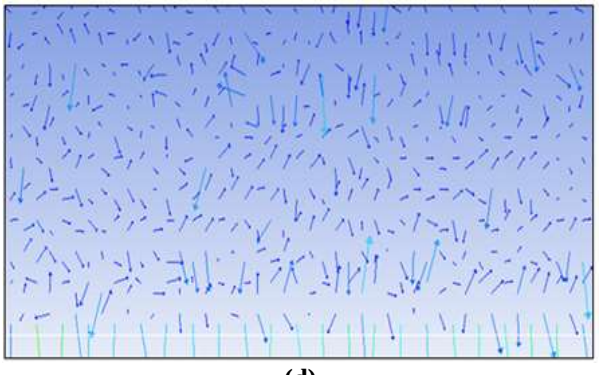

(d)

Fig. 10 Temperature distribution (K) at: (a): 8:00, (b): 13:00, and (c): 22:00 (second day). (d): velocity vector at 22:00 near the soil surface.

The above-mentioned method can be used for predicting the temperature distribution inside the greenhouse in different locations. As a case study, the temperature distribution is analyzed in Makran (latitude: 25.3054° N and longitude: 60.6411° E), a semi-desert coastal strip in Baluchestan, Iran, where studying agriculture in this region is significant [30]. The specified climatic conditions are used, considering conduction boundary conditions for inner surfaces and a uniform temperature at a depth of one meter in the soil. Figures 9 and 10 show the temperature contour at different times and the velocity vector near the south roof at certain times.

As seen in "Figs. 9 and 10", the temperature distribution inside the greenhouse varies at different times due to the time-dependent nature of the incident solar radiation flux. This capability to predict the climatic conditions within the greenhouse can provide valuable insights for optimizing crop production. Understanding how temperature fluctuations correlate with solar radiation over time allows for better management of growing conditions, enhancing the overall efficiency and yield of agricultural practices.

Figures 9 and 10(d) illustrate the fluid motion caused by natural convection due to the temperature differences inside the greenhouse. This highlights the significant role of natural convection in the heat transfer process,

influencing the temperature distribution within the solar greenhouse. As seen in "Figs. 9 and 10(b)", the variation in temperature distribution is significant at 13:00 on both the first and second days. Figure 11 shows the thermal variation along horizontal lines at different y-coordinate levels.

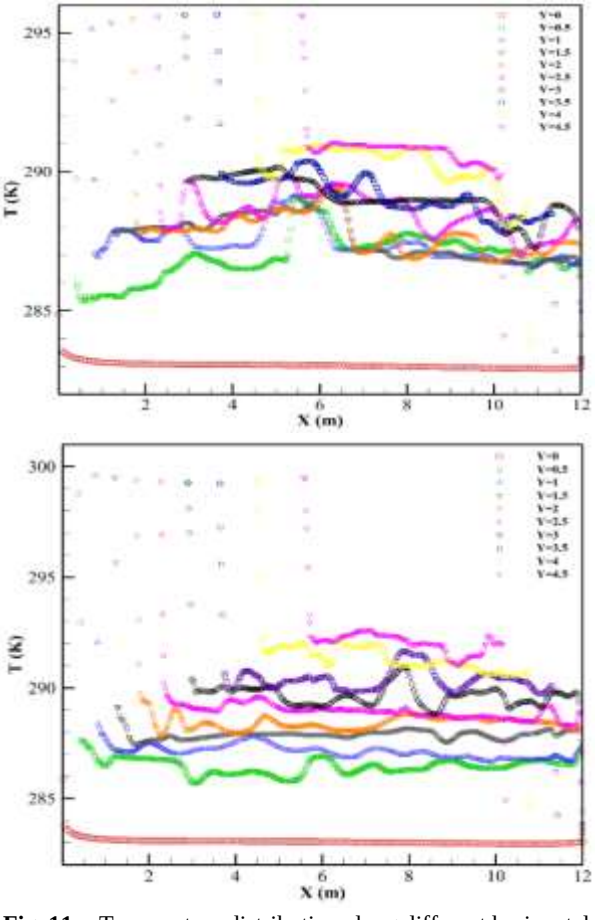

Fig. 11 Temperature distribution along different horizontal lines at: (a): 13:00 (first day), and (b): 13:00 (second day). The center of the coordinates is shown in "Fig. 1".

The variation in temperature distribution along these horizontal lines is evident in "Fig. 11", clearly indicating that the highest temperature occurs near the south roof. Visualizing the thermal distribution along different hypothetical horizontal lines inside the greenhouse is valuable for agricultural purposes in Makran, as it enables accurate prediction of thermal conditions.

4 CONCLUSIONS

This study utilizes the finite volume method with ANSYS Fluent to solve the continuity, Navier-Stokes, and energy Equations, aiming to model the climatic conditions inside a two-dimensional solar greenhouse. The Equations governing the solar radiation model and transient external climatic conditions are detailed and utilized to validate the study against experimental data. As a case study, the study predicts the temperature distribution inside a solar greenhouse in Makran, Iran. The transient nature of boundary conditions results in varying thermal conditions inside the greenhouse at different times. Furthermore, the findings reveal spatial variations in thermal distribution behavior. The research highlights the significant role of natural convection in influencing thermal distribution within the greenhouse. The results demonstrate the capability of the numerical method to accurately simulate the thermal behavior of solar greenhouses, as evidenced by the strong agreement between numerical predictions and experimental data. Consequently, accurate prediction of temperature distribution is crucial for advancing agricultural practices in solar greenhouses.

REFERENCES

[1] Tawalbeh, M., Aljaghoub, H., Alami, A., and Olabi, A., Selection Criteria of Cooling Technologies for Sustainable Greenhouses: A Comprehensive Review, Thermal Science and Engineering Progressy, Vol. 38, 2023, pp. 101666, https://doi.org/10.1016/j.tsep.2023.101666.

[2] Ding, D., Design Strategies of Passive Solar Greenhouses: A Bibliometric and Systematic Review, Ain Shams Engineering Journal, Vol. 15, No. 5, 2024, pp. 102680, https://doi.org/10.1016/j.asej.2024.102680.

[3] Garg, H. P., Advances in Solar Energy Technology, Volume 3 Heating, Agricultural and Photovoltaic Applications of Solar Energy (Softcover Reprint of the Original 1st ed. 1987), Springer Dordrecht, Netherlands, Chap. 5, 2011.

[4] Fatnassi, H., Bournet, P. E., Boulard, T., Roy, J. C., Molina-Aiz, F. D., and Zaaboul, R., Use of Computational Fluid Dynamic Tools to Model the Coupling of Plant Canopy Activity and Climate in Greenhouses and Closed Plant Growth Systems: A Review, Biosystems Engineering, Vol. 230, 2023, pp. 388–408, https://doi.org/10.1016/j.biosystemseng.2023.04.016.

[5] Okushima, L., Sase, S., and Nara, M., A Support System for Natural Ventilation Design of Greenhouse Based on Computational Aerodynamics, Acta Horticulturae, Vol. 248, No. 13, 1989, pp. 129–136, 10.17660/ActaHortic.1989.248.13.

[6] Sase, S., Takakura, T., and Nara, M., Wind Tunnel Testing on Airflow and Temperature Distribution of a Naturally Ventilated Greenhouse, Acta Horticulturae, Vol. 148, No. 42, 1984, pp. 329–336, 10.17660/ActaHortic.1984.148.42.

[7] Mistriotis, A., Bot, G. P., Boulard, T., Feuilloley, P., Papadakis, G., Picuno, P., and Scarascia-Mugozza, G.,

New Techniques in Greenhouse Ventilation Analysis, AGENG 96 International Conference on Agricultural Engineering, Madrid, 1996, pp. 392–393.

[8] Bartzanas, T., Boulard, T., and Kittas, C., Numerical Simulation of the Airflow and Temperature Distribution in a Tunnel Greenhouse Equipped with Insect-Proof Screen in the Openings, Computers and Electronics in Agriculture, Vol. 34, 2002, pp. 207–221, 10.1016/S0168-1699(01)00188-0.

[9] Molina-Aiz, F. D., Valera, D. L., and Alvarez, A. J., Measurement and Simulation of Climate inside Almería-Type Greenhouses using Computational Fluid Dynamics, Agricultural and Forest Meteorology, Vol. 125, 2004, pp. 33–51, 10.1016/j.agrformet.2004.03.009.

[10] Tong, G., Christopher, D. M., and Li, B., Numerical Modelling of Temperature Variations in a Chinese Solar Greenhouse, Computers and Electronics in Agriculture, Vol. 68, 2009, pp. 129–139, 10.1016/j.compag.2009.05.004.

[11] Rodriguez, C. E. A., Velazquez, J. F., Heat and Mass Transfer - Advances in Science and Technology Applications, 1st ed., Intech Open, London, United Kingdom, Chap. 6, 2019.

[12] Sadodin, S., Kashani, T., Numerical Investigation of a Solar Greenhouse Tunnel Drier for Drying of Copra, arXiv preprint arXiv: 1102.2522, 2011, 10.48550/arXiv.1102.4522.

[13] Lokeswaran, S., Eswaramoorthy, M., An Experimental Analysis of a Solar Greenhouse Drier: Computational Fluid Dynamics (CFD) Validation, Energy Sources, Part A: Recovery, Utilization, and Environmental Effects, Vol. 35, No. 21, 2013, pp. 2062–2071, 10.1080/15567036.2010.532195.

[14] Deiana, A., Fabrizio, E., and Gerboni, R., Energy Performance Optimization of Typical Chinese Solar Greenhouse by Means of Dynamic Simulation, International Conference on Agriculture Engineering, Zurich, 2014, pp. 1–8.

[15] Chen, C., Ling, H., Zhai, Z., Li, Y., Yang, F., Han, F., and Wei, S., Thermal Performance of An Active-Passive Ventilation Wall with Phase Change Material in Solar Greenhouse, Applied Energy, Vol. 216, 2018, pp. 602–612, 10.1016/j.apenergy.2018.02.130.

[16] Tong, G., Christopher, D. M., Sensitivity Analysis of the Air Temperature Variations in a Chinese Solar Greenhouse, Acta Horticulturae, Vol. 1170, 2017, pp. 71–78, 10.17660/ActaHortic.2017.1170.7.

[17] He, X., Wang, J., Guo, S., Zhang, J., Wei, B., Sun, J., and Shu, S., Ventilation Optimization of Solar Greenhouse with Removable Back Walls Based on CFD, Computers and Electronics in Agriculture, Vol. 149, 2018, pp. 16–25, 10.1016/j.compag.2017.10.001.

[18] Esmaeli, H., Roshandel, R., Optimal Design for Solar Greenhouses Based on Climate Conditions, Renewable Energy, Vol. 145, 2020, pp. 1255–1265, 10.1016/j.renene.2019.06.090.

[19] Currie, I. G., Fundamental Mechanics of Fluid, 3rd ed., Marcel Dekker Inc., New York, USA, 2003, pp. 3–40.

[20] ANSYS, ANSYS Fluent User's Guide, Ver. 12, Canonsburg, Pennsylvania, USA, 2009.

[21] Yang, D. K. W., Abakr, Y. A., and Ghazali, N. M., CFD Investigation of the Heat Transfer between an External Heat Source and the Regenerator of a Thermoacoustic Engine, Procedia Engineering, Vol. 56, 2013, pp. 835–841, 10.1016/j.proeng.2013.03.204.

[22] Berdahl, P., Fromberg, R., Thermal Radiance of Clear Skies, Solar Energy, Vol. 29, 1982, pp. 299–314.

[23] Alizadeh, A., The Principles of Applied Hydrology, 36th ed., Imam Reza (AS) University, Mashhad, Iran, 2013.

[24] Tiwari, G. N., Solar Energy Fundamentals, Design, Modelling and Applications, 1st ed. Narosa, New Delhi, India, 2002.

[25] Duffie, J. A., Beckman, W. A., Solar Engineering of Thermal Process, 4th ed., John Wiley & Sons, Inc. Hoboken, New Jersey, 2013.

[26] Padilla, R. V., Simplified Methodology for Designing Parabolic through Solar Power Plants, Ph.D. Dissertation, Department of Chemical and Biomedical Engineering, University of South Florida, Tampa, Fl, Apr. 2011.

[27] Garzoli, K., A Simple Greenhouse Climate Model, Acta Horticulturae, Vol. 174, 1985, pp. 393–400, 10.17660/ActaHortic.1985.174.52.

[28] Garzoli, K. V., Blackwell, I., An Analysis of the Nocturnal Heat Loss from a Single Skin Plastic Greenhouse, Journal of Agricultural Engineering Research, Vol. 26, No. 3, 1981, pp. 204–214, 10.1016/0021-8634(81)90105-0.

[29] Baille, A., Lopez, J. C., Bonachela, S., Gonzalez-Real, M. M., and Montero, J. I., Night Energy Balance in a Heated Low-Cost Plastic Greenhouse, Agricultural and Forest Meteorology, Vol. 137, 2006, pp. 107–118, 10.1016/j.agrformet.2006.03.008.

[30] Noorisameleh, Z., Gough W. A., The Challenge of Climate Change in Agriculture Management in the Persian Gulf-Oman Sea Coasts in Iran, Transforming Coastal Zone for Sustainable Food and Income Security. Springer, Cham, 2022, pp. 887–893.